WIND TUNNEL TESTS OF THE SM701 AIRFOIL AND THE UAG 88-143/20 AIRFOIL

by D.Althaus and W.Wurz
Institut fur Aerodynamik und Gasdynamik, Universitat Stuttgart

The SM701 airfoil was designed by Dan M.Somers and Mark D. Maughmer to be applied on World Class sailplanes. [1] Main objectives in the design of the 16 per cent thick laminar flow airfoil have been high maximum lift, low profile drag and docile stall. A model was tested in the Laminar Wind Tunnel of the University of Stuttgart at Reynolds numbers of 0.7,1.0, 1.5 and 2.5 million and at a Reynolds number of 1.5 million with simulated roughness.

The UAG88-143/20 airfoil was designed by D.J.Marsden[2] to be used on an ultralight sailplane wing. A model was tested in the low turbulence wind tunnel of the University of Alberta. The test results show a suprisingly good performance. They are compared with the polars of the FX 67-K-150/17 wing section, which was tested among a lot of other sections in the Laminar Wind Tunnel of the University of Stuttgart. To compare with the results of the University of Alberta, it was decided to test the UAG 88-143/20 section in the same tunnel.

WIND TUNNEL

The Laminar Wind Tunnel of the Institute is built as an open return tunnel of the Eiffel design.[3] The high contraction ratio of 100:1 and screens result in a very low turbulence level of less than $2 \cdot 10^{-4}$. The rectangular test section measures 0.73 m x 2.73 m and is 3.15 m long. The two

dimensional airfoil models span the short distance of the test section. Blowing air tangential in the corner between the model and the mounting plates is used as a boundary layer control to ensure two-dimensional conditions.

The lift is determined by integration of the pressure distribution along the tunnel walls. The drag is determined by an integrating rake which is 0.3 chord lengths behind the model trailing edge. Both integrations are made experimentally. As demonstrated in[4] longitudinal vortices sometimes produce periodical variations of drag. The pressure readings of the rake are therefore integrated while traversing the rake along 0.3 m of the model span.

The pitching moment is determined by the mechanical torsion about the quarter chord pivot point. The data acquisation system is controlled by a computer which also performs the calculations to determine the aerodynamic coefficents including standard wind tunnel corrections and which disposes the coefficients on-line on a plotter. The system is triggered with a frequency of about 5 Hz with the plotter pen in the pen-up position. Thus, the form of the drag polar can easily be controlled when the angle of attack of the model is varied. By pressing a knob, integration of the drag along the span is initiated and the resulting coefficients are marked on the plotter and stored by the computer.

Before each test the whole system is calibrated by simulating the pressures for lift and drag by high precision pressures which are produced by the immersed-jar principle. After the calibration for one set of pressures, the correct response of the system is checked by applying different pressure sets.

Standard model chords range from 0.5 m to 1.0 m and result in Reynolds numbers between $0.7 \cdot 10^6$ and $5.5 \cdot 10^6$. The corresponding pressures are in a range which can be measured with sufficient accuracy.

The transition of boundary layers is detected by a stethoscope or by flow visualisation. A mixture of petrol and lamp-black is used to mark the transition and laminar separation bubbles on the white painted models.

To simulate a pattern of insects, 10 mm wide strips of Mylarfilm, 0.06 mm thick with bumps of a half-spherical form in a distance of 30 mm and 0.5 mm high are used. One of these strips is fastened on the airfoil nose in such a way that the bumps are directly in the nose line. One strip is tightly fixed at the pressure side and two other strips are so tightly fixed on the suction side of the airfoil nose that the bumps are shifted spanwise half of their distance from strip to strip. The second one of these two strips is 30 mm wide with the bumps in its middle. This pattern is thought to agree with reality. As the strips can easily be produced and and fixed, the pattern is easily reproduceable.

MODEL CONSTRUCTION

The models are built of Polyurethane-Foam and fibre glass. Two templates are cut by a computer-controlled laser beam. The strongly focussed laser beam only causes a very small gap. Thus, a positive as well as a negative template are available to control the correct model shape. The foam is sanded down to the templates, coated with thin sheets of fibre glass and painted. The surface is smoothed by wet sanding with 1200 grit sandpaper and polishing.

The airfoil shapes are within 0.3mm as controlled by the negative template (0.06% of chord).

SM 701 AIRFOIL: TESTS AND RESULTS

The coordinates of the airfoil are listed in Table 1. The shape of the SM701 wing section is shown in Figure 1 and the inviscid velocity distribution in Figure 2. The chord of the model was 0.5 m. The tunnel wall blowing was installed at 60% of chord on the suction side of the model.

SM701 AIRFOIL COORDINATES

Upper Surface		Lower Surface	
x/c	y/c	x/c	y/c
0.00168	0.00771	0.00016	−0.00212
.00736	.01910	.00435	−.00981
.01701	.03121	.01501	−.01632
.03055	.04344	.03127	−.02244
.04794	.05534	.05277	−.02800
.06915	.06648	.07923	−.03294
.09417	.07658	.11036	−.03726
.12295	.08544	.14575	−.04101
.15541	.09296	.18488	−.04418
.19133	.09914	.22722	−.04670
.23041	.10397	.27222	−.04849
.27229	.10746	.31929	−.04943
.31654	.10964	.36784	−.04938
.36268	.11055	.41726	−.04803
.41019	.11018	.46727	−.04488
.45853	.10853	.51811	−.03983
.50714	.10557	.56979	−.03340
.55548	.10120	.62191	−.02623
.60323	.09517	.67386	−.01887
.65041	.08760	.72497	−.01182
.69676	.07903	.77446	−.00553
.74171	.06990	.82144	−.00041
.78466	.06055	.86497	.00324
.82498	.05125	.90406	.00526
.86207	.04221	.93768	.00567
.89529	.03348	.96489	.00463
.92431	.02493	.98462	.00262
.94922	.01669	.99624	.00073
.96999	.00946	1.00000	.00000
.98605	.00405		
.99640	.00095		
1.00000	.00000		

TABLE 1.

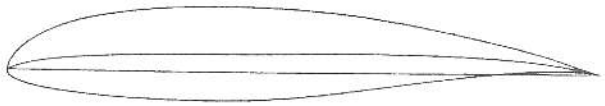

FIGURE 1. Shape of SM701 airfoil.

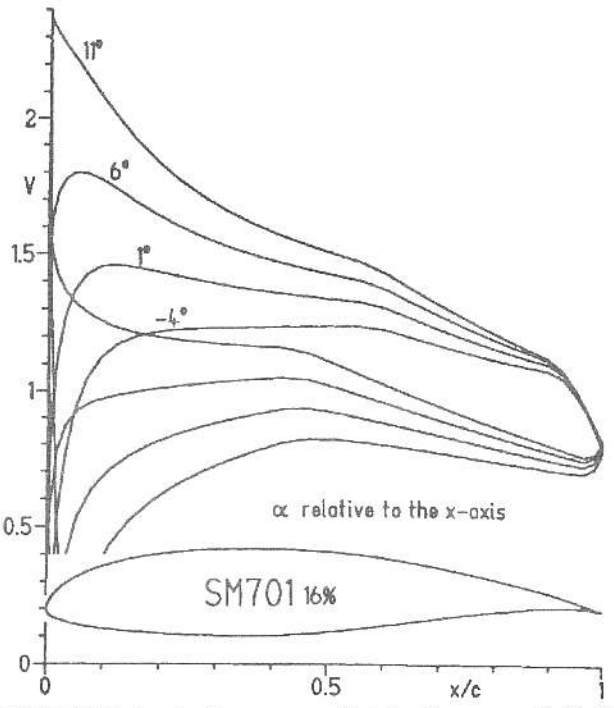

FIGURE 2. Inviscid pressure distribution; $\alpha = -4°, 1°, 6°, 11°$ from Ref. 1.

Figure 3 shows the polars as tested in the wind tunnel. The theoretical polars are calculated with the Eppler code and tabulated in listings[1]. In Figure 4 polars from the wind tunnel, Eppler code and Drela-XFOIL-code at RN = 0.7 • 10^6 are shown for comparison. The Drela-XFOIL-code[5] is a method for analysing airfoils with transitional separation bubbles in a viscous/inviscid manner. The drag coefficients calculated by the two codes are nearly identical but less than the measured ones. The lower and the upper corner of the drag bucket of the XFOIL code and measurement roughly agree with each other while the Eppler code predicts a bucket which is essentially too wide. The lift curve slope predicted by XFOIL is too flat for $\alpha > 2$ degrees and too steep for $\alpha < 6$ degress as calculated by the Eppler code.

The same statements hold for RN = 1.0 • 10^6 as shown in Figure 5. In addition this figure shows the variation of the transition locations as calculated by the two codes. The position of laminar separation bubbles as taken from flow visualisation at zero angle of attack (Figure 6) is marked by barks. On the suction side a separation bubble extents from 60% to 66% of the chord, on the pressure side from 50% to 62%. XFOIL shows transition at 67% of the chord without a laminar separation bubble on the suction side while a separation bubble between 51% and 62% is predicted for the pressure side. This is nearly identical with the position detected by flow visualization. XFOIL handles a laminar separation bubble in an inverse mode of boundary layer calculation. The Eppler code switches from laminar to turbulent calculation when it detects transition or laminar separation. Transition as indicated by the Eppler code coincides with experimental separation. Despite these differences both codes calculate nearly equal drag coeffi-

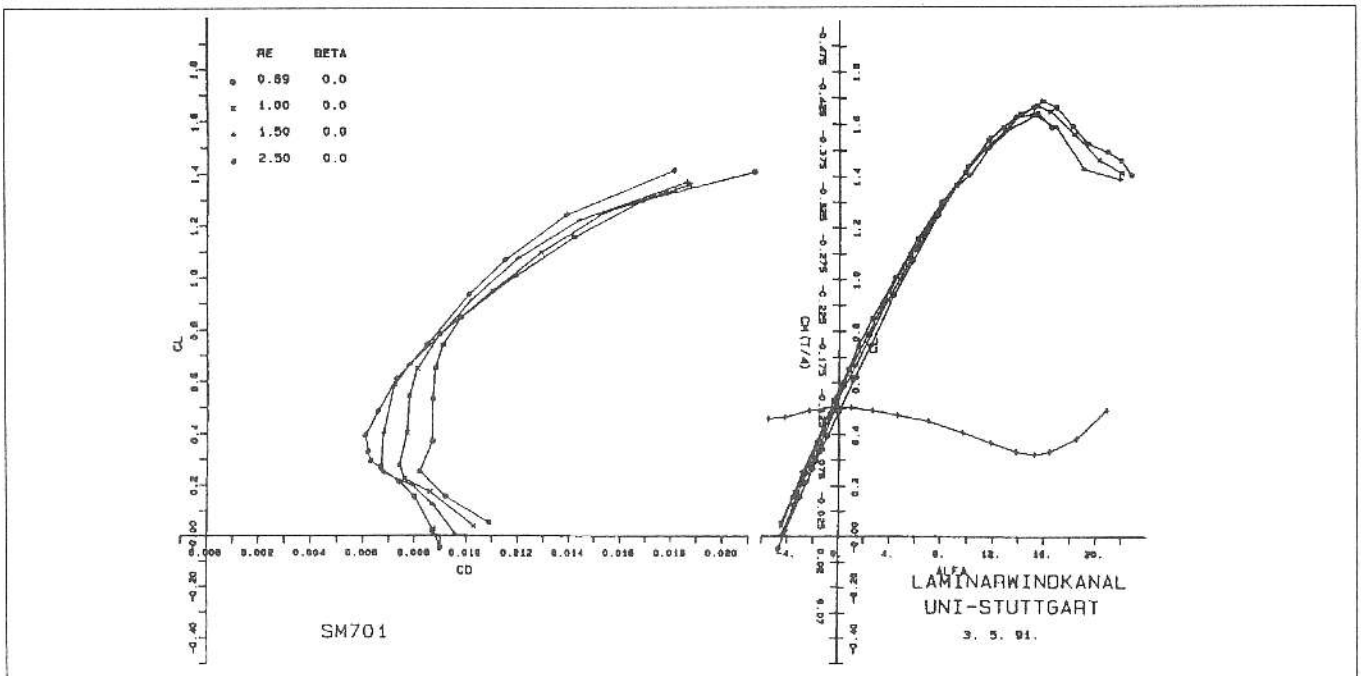

FIGURE 3. Wind tunnel results C_L vs C_D, C_L vs α; RN = 0.7 • 10^6, 1.0 • 10^6, 1.5 • 10^6, 2.5 • 10^6; Cm vs α; RN = 1.5 = 10^6.

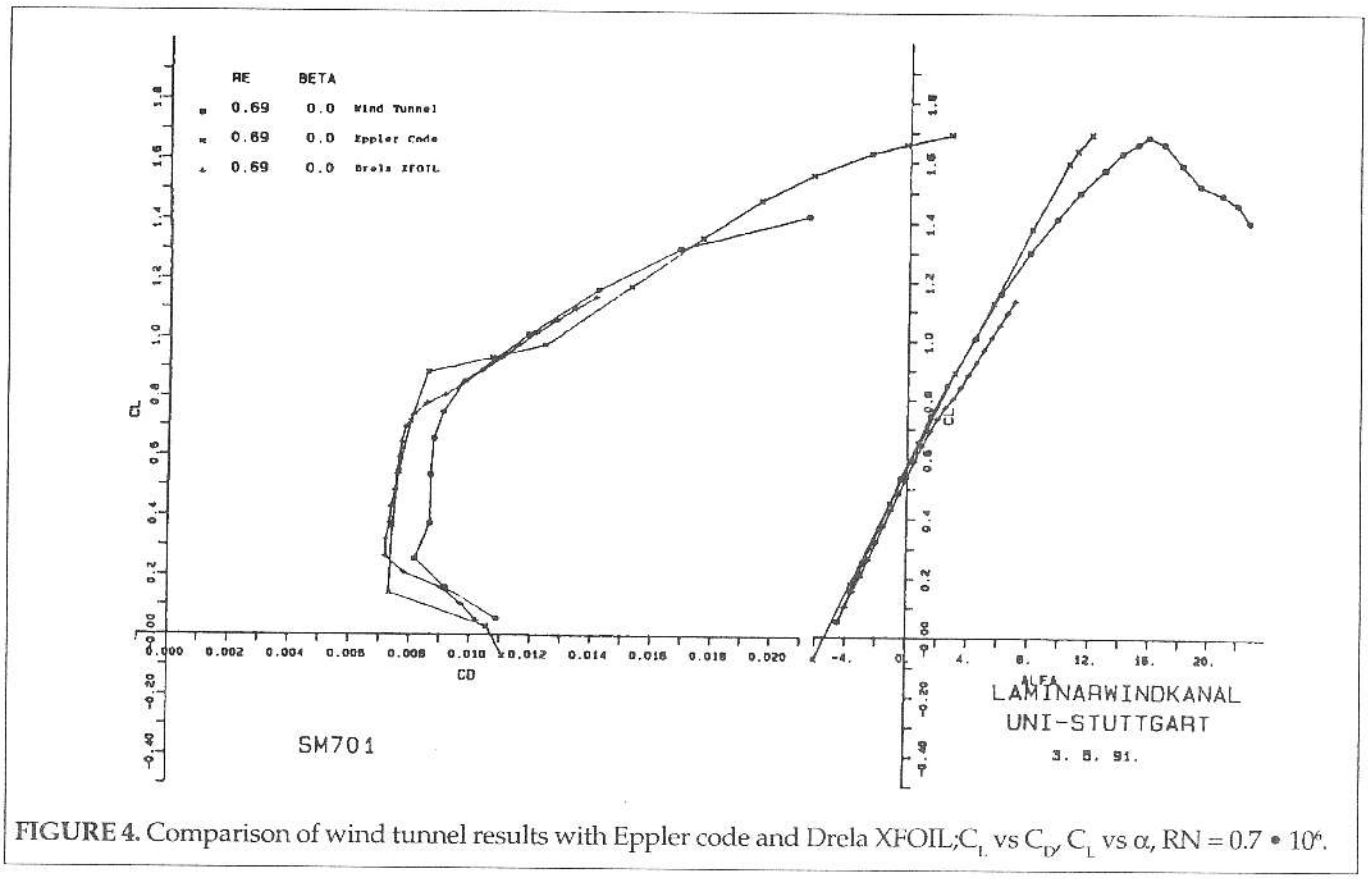

FIGURE 4. Comparison of wind tunnel results with Eppler code and Drela XFOIL;C_L vs C_D, C_L vs α, RN = 0.7 • 10^6.

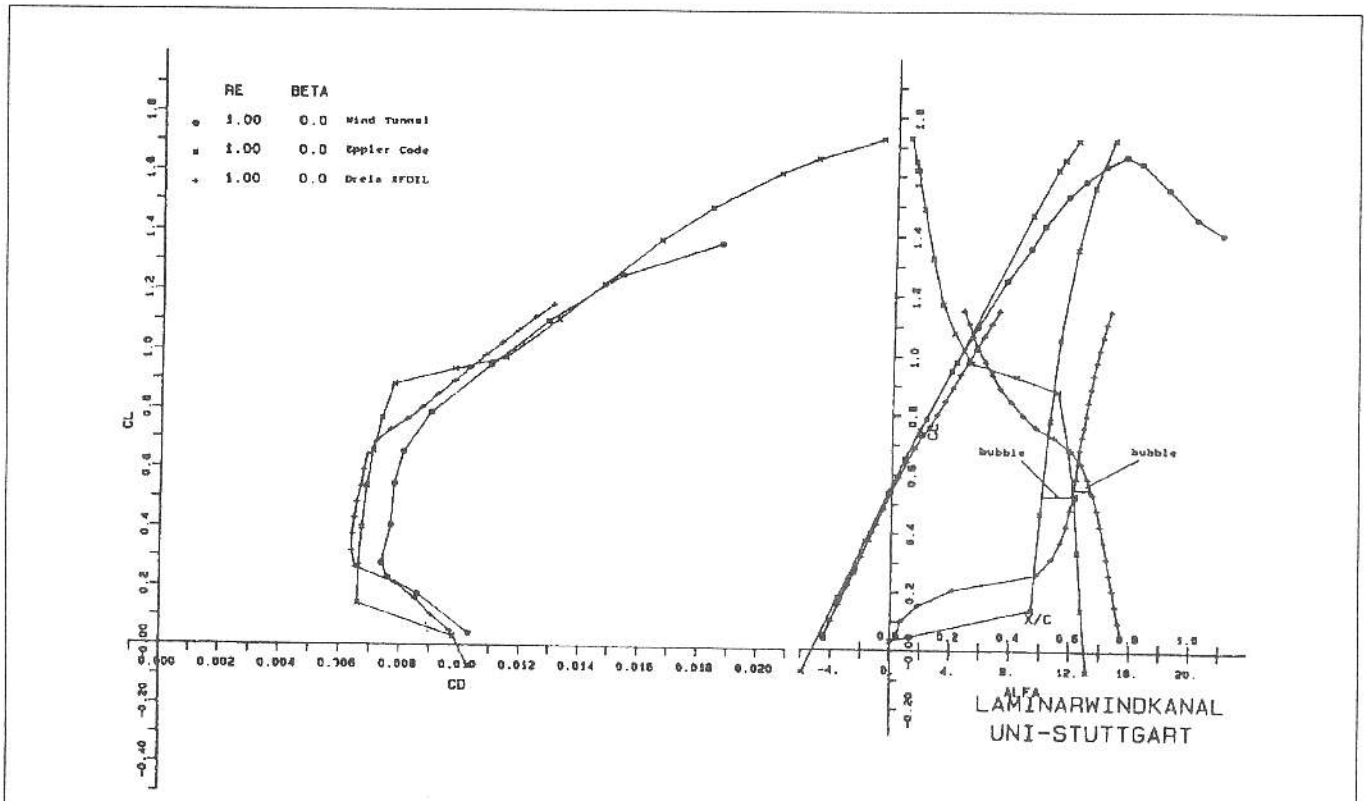

FIGURE 5. Comparison of wind tunnel results with Eppler code and Drela XFOIL; C_L vs C_D, C_L vs α, RN = 1.0 • 106; transition positions from Eppler code and Drela XFOIL position of laminar separation bubble from oil film technique

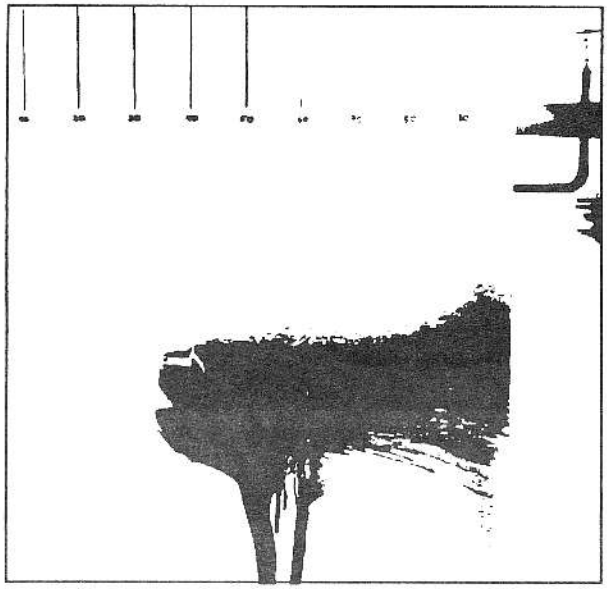

FIGURE 6. Flow visualization by the oilfilm technique on the pressure side of the vertical mounted model. Flow direction from left to right; $\alpha = 0°$, RN = 1.0 • 10^6.

cients between $C_L = 0.25$ and $C_L = 0.7$.

In Figure 7 the lift-drag polars for RN = 1.5 • 10^6 show similar behaviour as in previous cases. The Eppler code calculates a higher pitching moment while the results from XFOIL are somewhat too low. At RN = 2.5 • 10^6, see Figure 8, the difference between the minimum drag coefficient predicted by the Eppler code and measurement is smaller. The XFOIL code calculates a low drag range similar to the measured one but at some higher lift coefficients. Figure 9 shows polars for RN = 1.5 • 10^6 measured with roughness which is produced by the bug pattern described above and calculated by the Eppler code with a special transition mode.[1]

CONCLUDING REMARKS

The measured drag coefficients are higher than those which are calculated by the two codes. The low drag bucket from the measurements becomes essentially smaller with growing Reynolds numbers than predicted by the Eppler code. The XFOIL code, however, has the same tendency like the measurements. The differences between theoretical and experimental results are due to the existence of separation bubbles (Eppler code) and the different methods for the calculation of the turbulent boundary layers in both codes.

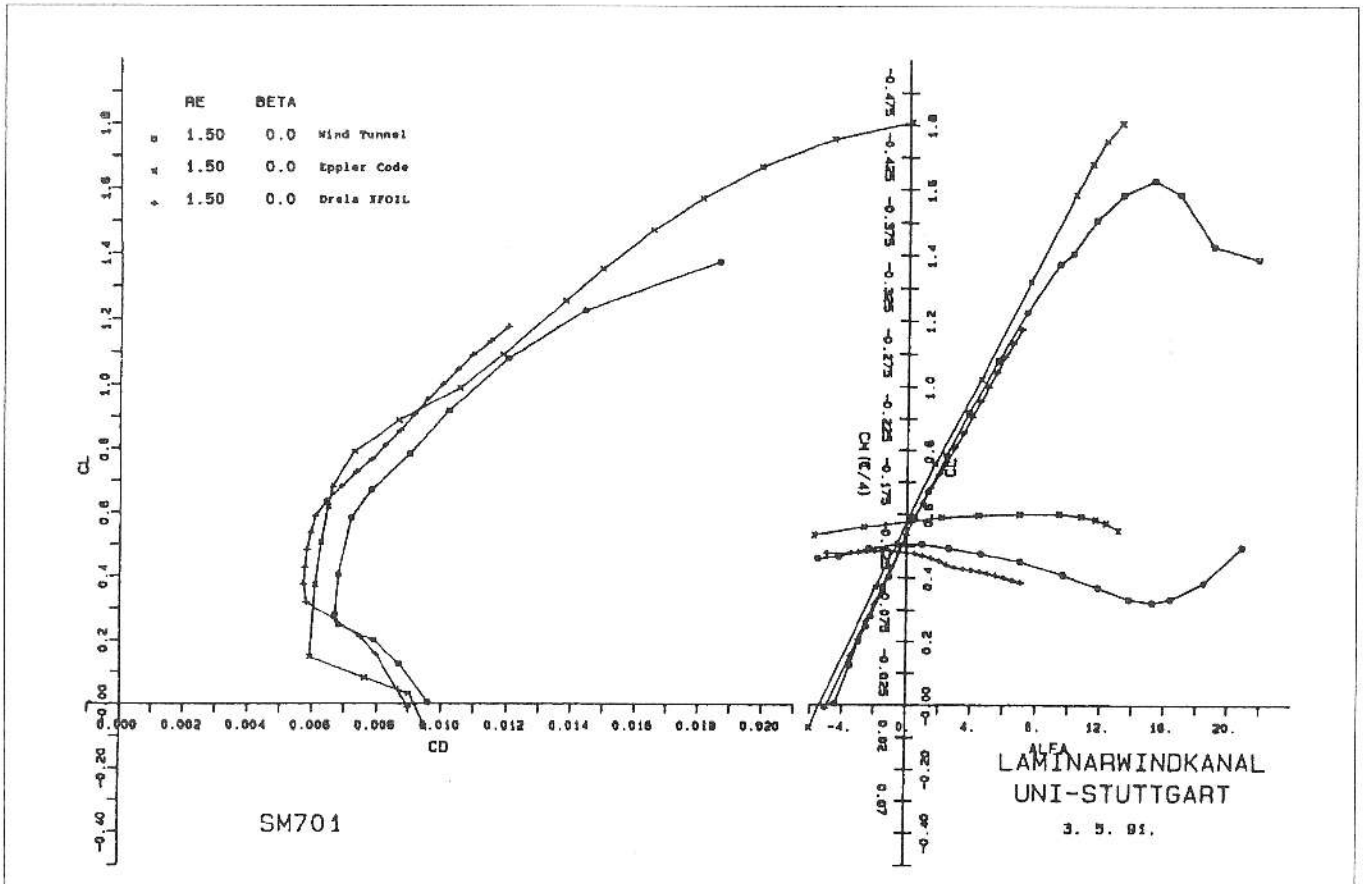

FIGURE 7. Comparison of wind tunnel results with Eppler code and Drela XFOIL; C_L vs C_D, C_L vs α, RN = 1.5 • 10^6.

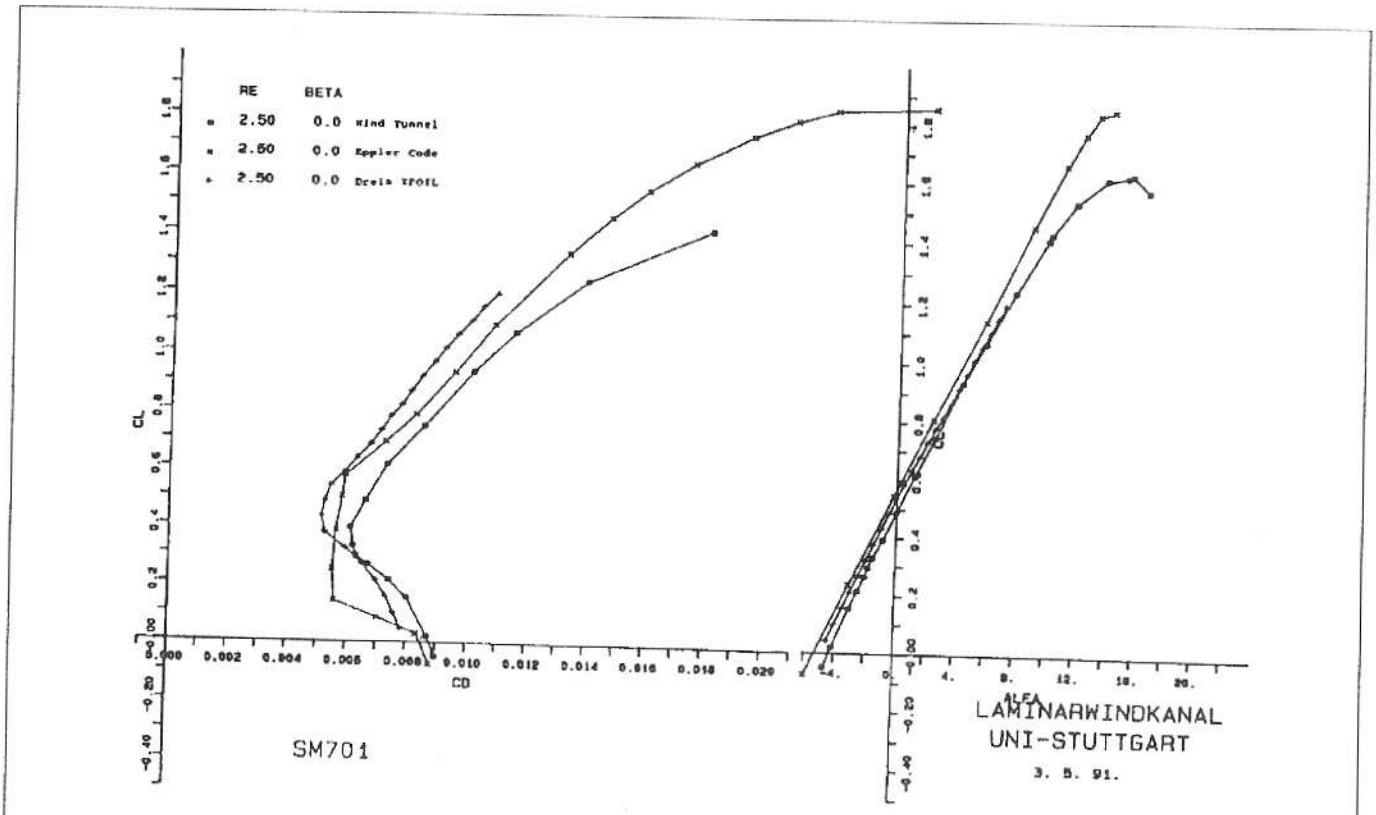

FIGURE 8. Comparison of wind tunnel results with Eppler code and Drela XFOIL; C_L vs C_D, C_L vs α, RN = 2.5 • 10^6.

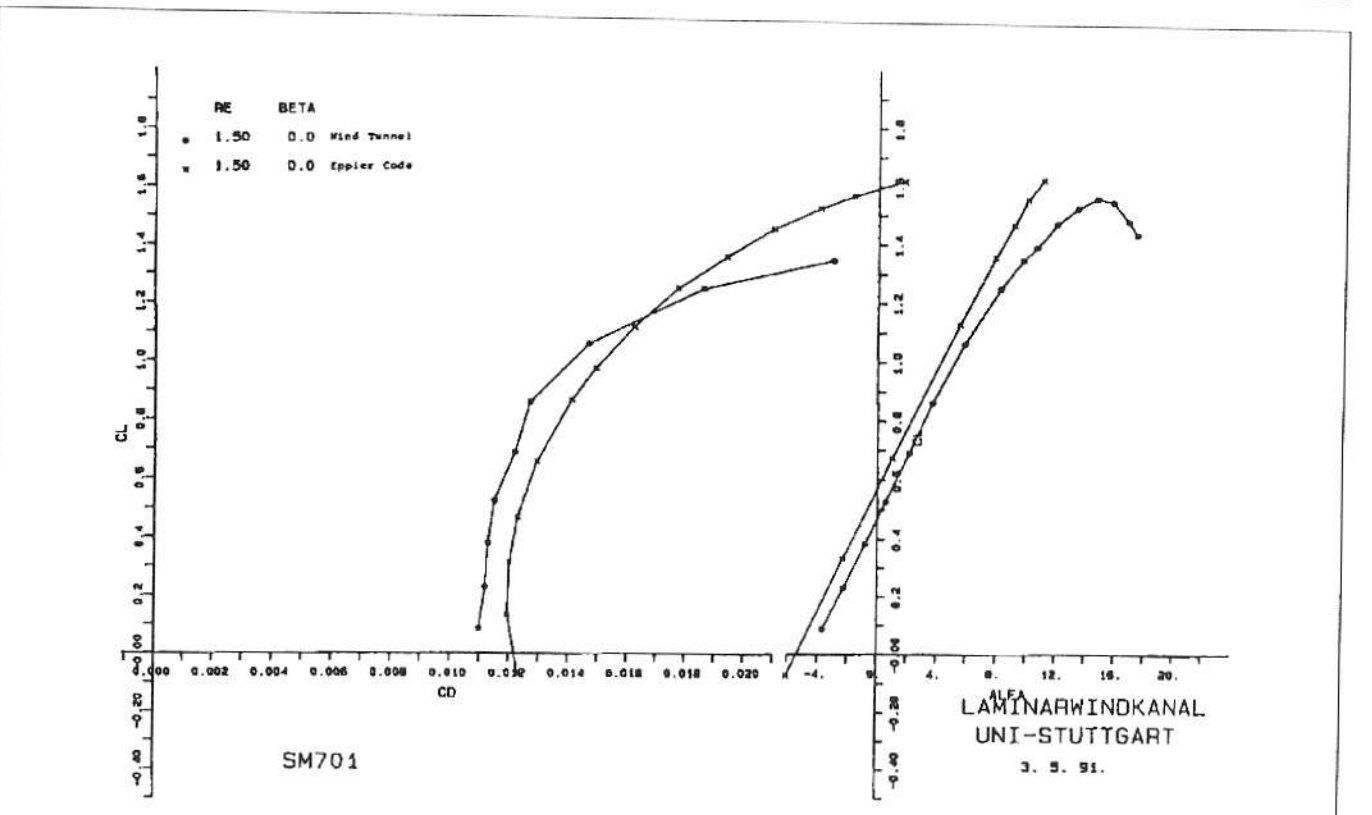

FIGURE 9. Airfoil with simulated insect roughness. Comparison of wind tunnel results and Eppler code. C_L vs C_D, C_D vs α, RN = 1.5 • 10^6.

UAG 88-143/20 AIRFOIL: WIND TUNNEL AND MODEL OF THE UNIVERSITY OF ALBERTA

The wind tunnel of the University of Alberta[2] is a closed return wind tunnel with test section dimensions of 1.22m x 2.44m. Its free-stream turbulence level is claimed[2] to be less than 0.01%.In an earlier paper[6] a value of 0.1% was given. This value is more reasonable for a closed return wind tunnel.

The lift and moment coefficients were determined by integration of measured pressure distributions. The drag was determined from a pitot-static traverse through the wake at a location of 1.5 chord lengths behind the model trailing edge. Boundary layer control by suction through a distribution of holes in the mounting plates at the end of the model was used to ensure two dimensional test conditions.

The model had a chord of 1 m and was tested at Reynolds numbers of $0.5 \cdot 10^6$, $1.0 \cdot 10^6$ and $2.1 \cdot 10^6$. This means free stream dynamic heads of 3.5, 14.1 and 62.4 mm water gauge. Measuring pressure distributions of the model and pressures in the wake 1.5 m behind the model at these very low pressures is a very difficult and uncertain procedure. The lowest free stream dynamic pressure attained in the Stuttgart tests was a water column of 27.5 mm at a Reynolds number of $0.7 \cdot 10^6$. Integrations of the pressures are performed experimentally. The Stuttgart model of the UAG 88-143/20 section had a chord of 0.5m. The 20% chord plain flap was constructed according to the Alberta model (see Figure 10).

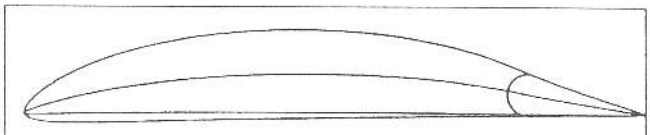

FIGURE 10. Shape of airfoil UAG 88/143/20.

RESULTS

Figures 11 to 14 show $C_L(C_D)$ and $C_L(\alpha)$ polars for Reynolds numbers of $0.7 \cdot 10^6$, $1.0 \cdot 10^6$, $1.5 \cdot 10^6$ and $2.1 \cdot 10^6$ respectively and various flap settings. At $\alpha = 1°$ and +10° flap setting a laminar separation bubble between 64% and 76% of chord on the suction side was detected by the oil film technique.

It is marked in Figure 11 for RN = $0.7 \cdot 10^6$. At RN = $1.0 \cdot 10^6$ the bubble is between 64% and 74% (se Figure12). Polars for RN = $1.5 \cdot 10^6$ are shown in Figure 13. At RN = $2.1 \cdot 10^6$ and zero flap setting a bubble is detected between 61% and 68% on the suction side for $\alpha = 2°$ (see Figure14) while for $\alpha = 4°$ transition takes place before the separation of the laminar boundary layer. The separation of the turbulent boundary layer is indicated at 98% of chord.

Pitching moments about the quarter chord of the airfoil and for the flap about its pivot point are shown in Figure15 for flap settings of 0.0°, 10° and -10° at RN = $2.1 \cdot 10^6$.

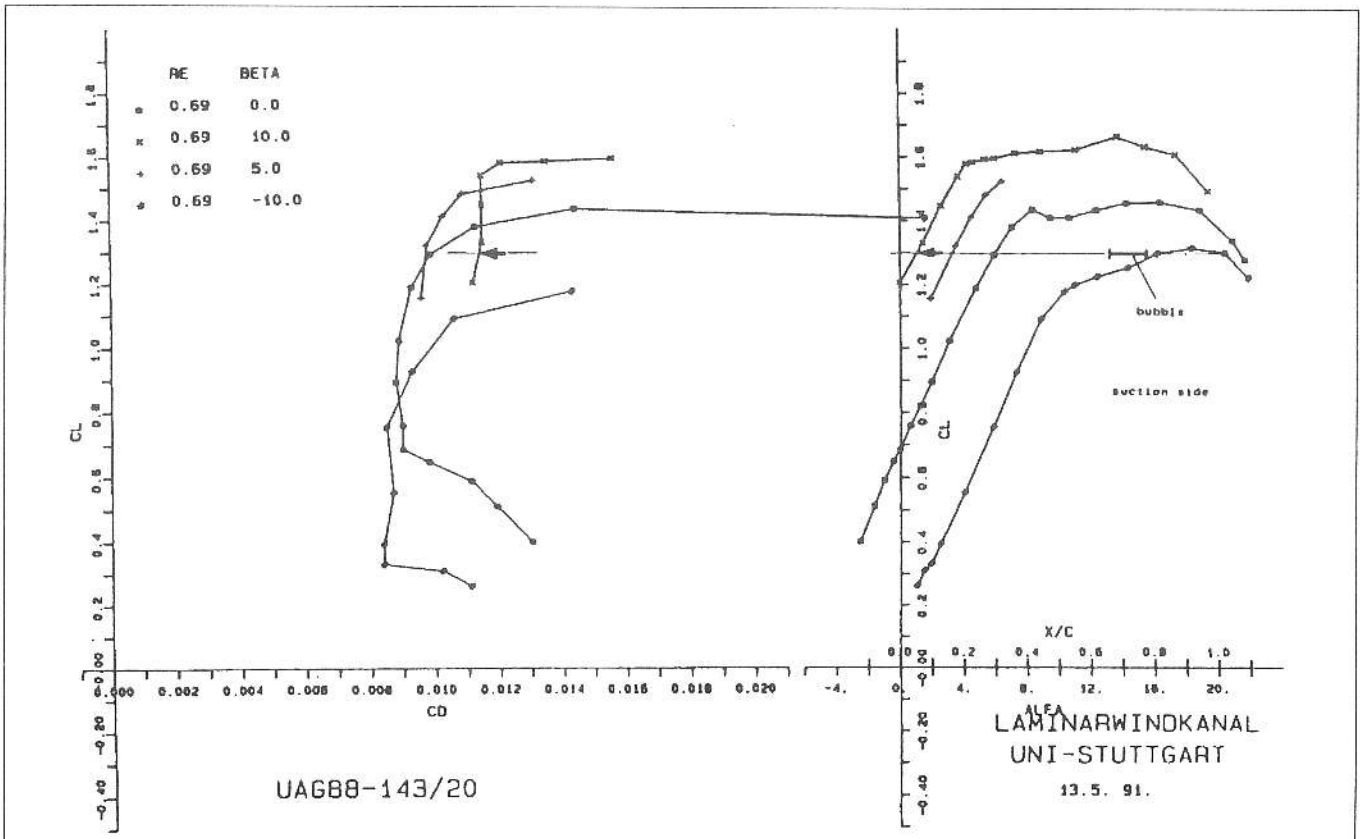

FIGURE 11. Polars at RN = $0.7 \cdot 10^6$ with position of a laminar separation bubble on the suction side, 10° flap deflection.

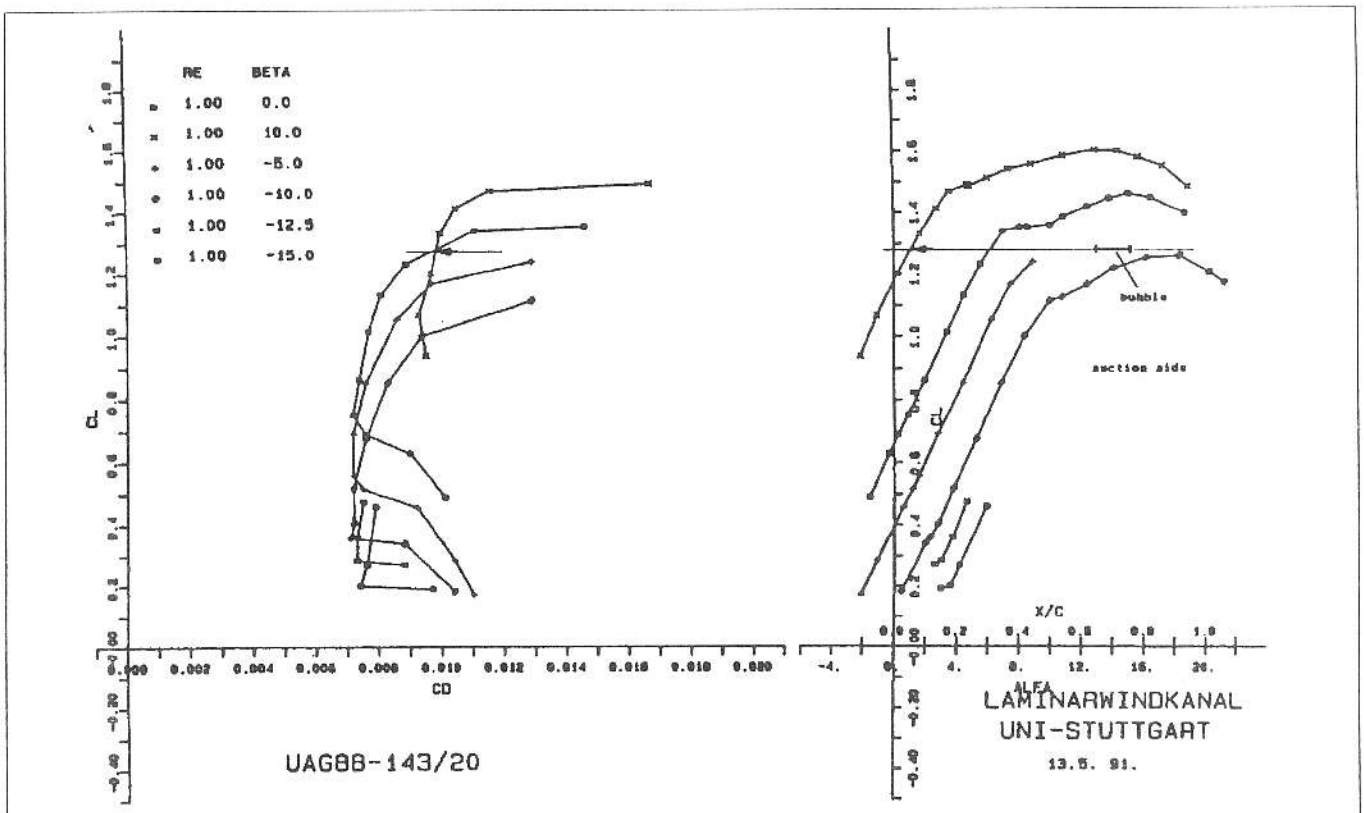

FIGURE 12. Polars at RN = 1.0 • 10^6 with postion of a laminar separation bubble on the suction side, 10° flap deflection.

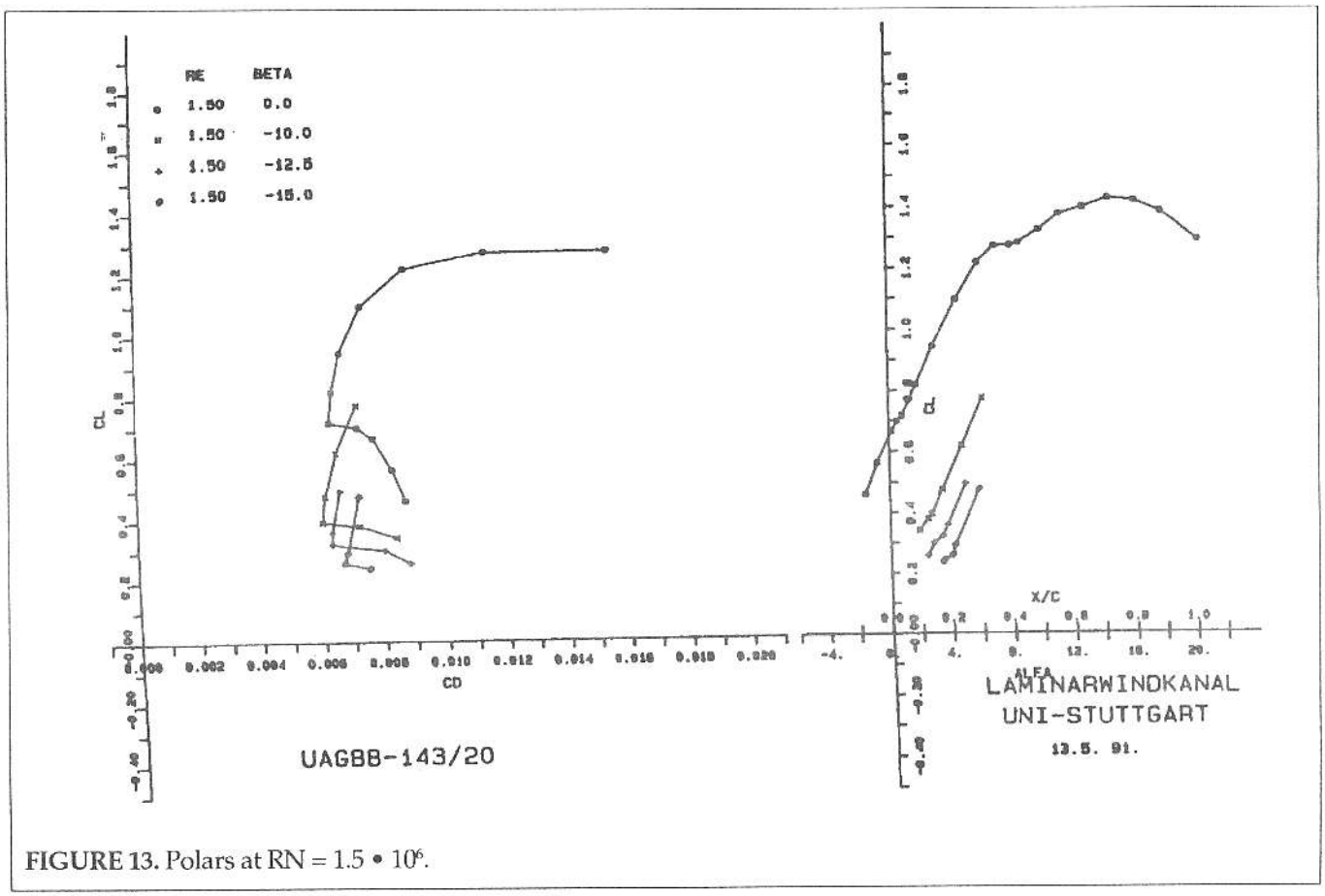

FIGURE 13. Polars at RN = 1.5 • 10^6.

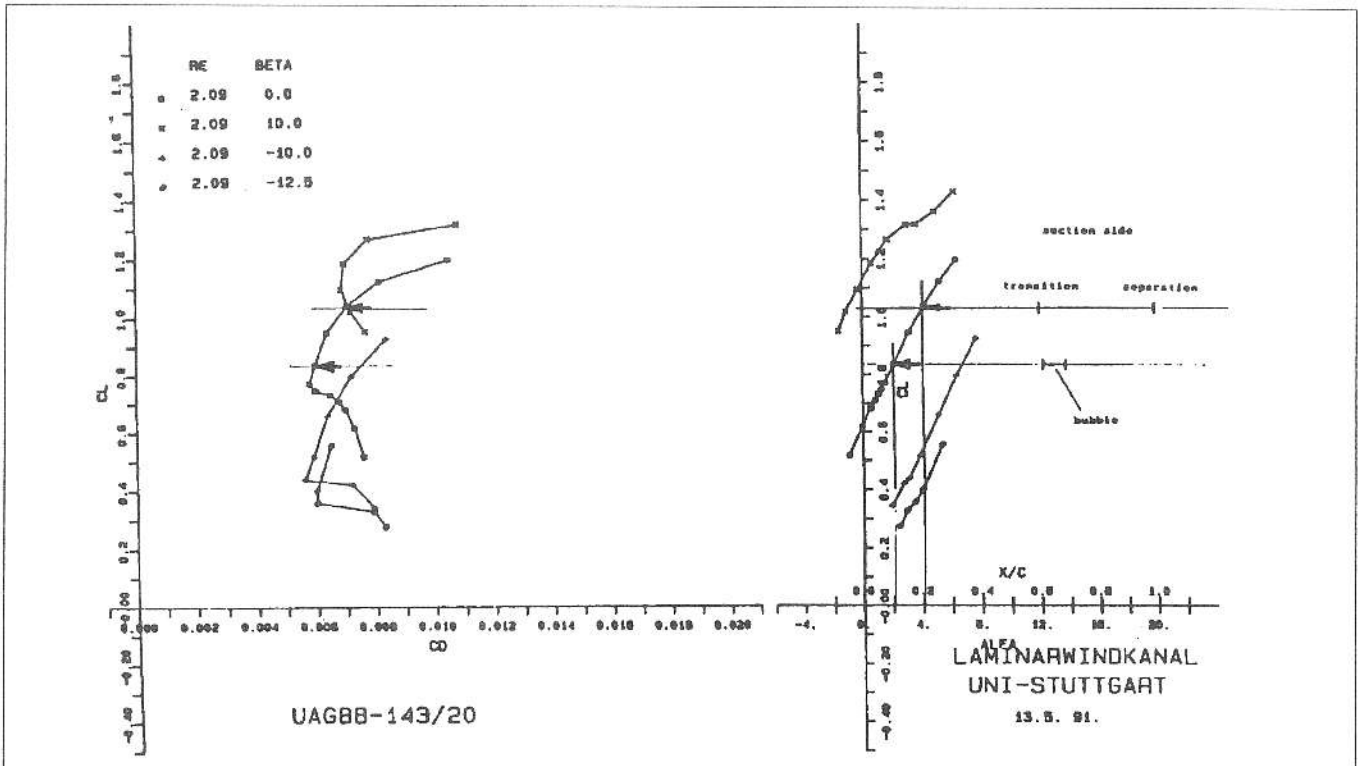

FIGURE 14. Polars at RN = 2.0 • 10^6 with position of a laminar separation bubble on the suction side at zero flap deflection for $\alpha = 2°$. Transition without laminar separation and turbulent separation near the trailing edge at $\alpha = 4°$.

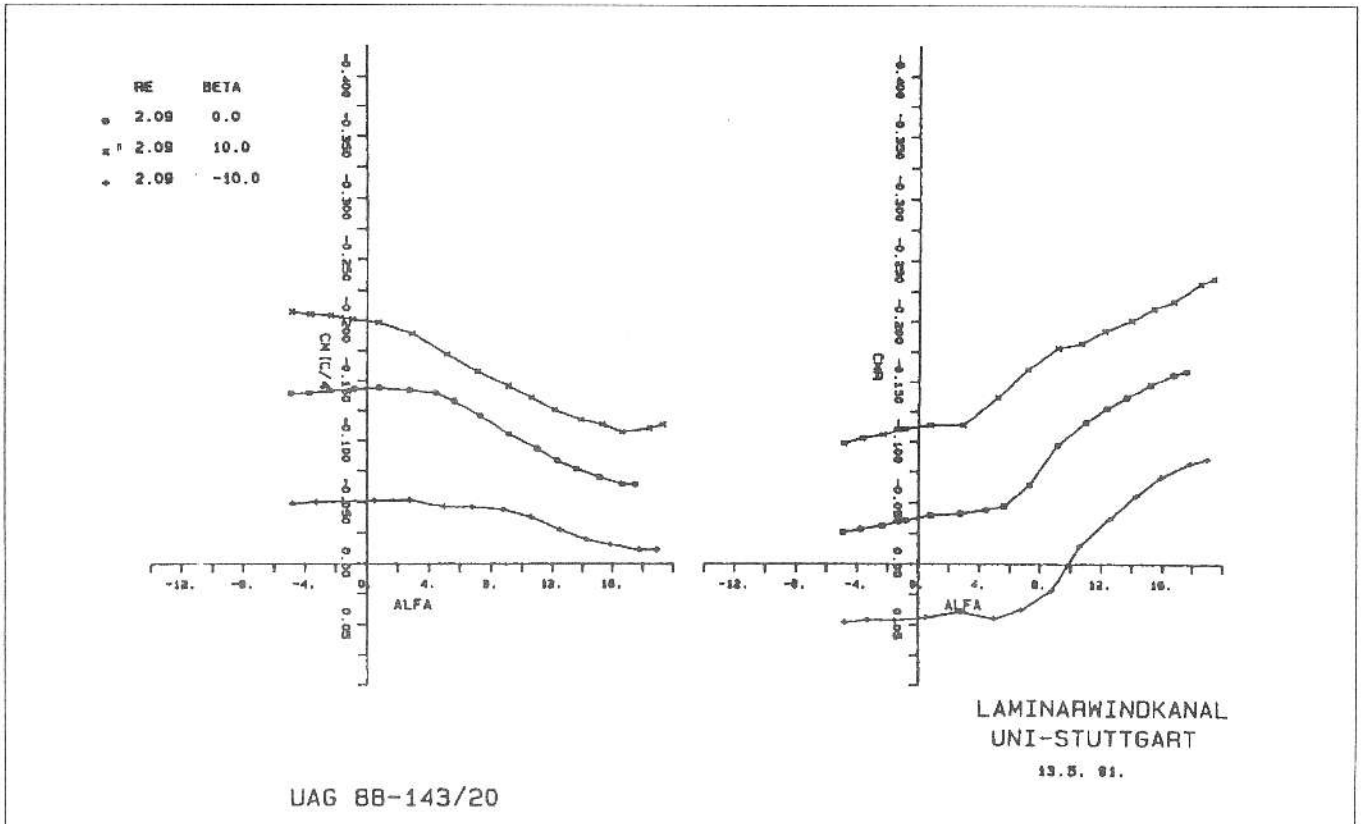

FIGURE 15. Moment coefficient of the airfoil about the quarter chord point. Moment coefficient of the flap about its pivot point based on flap chord. RN = 2.1 • 10^6.

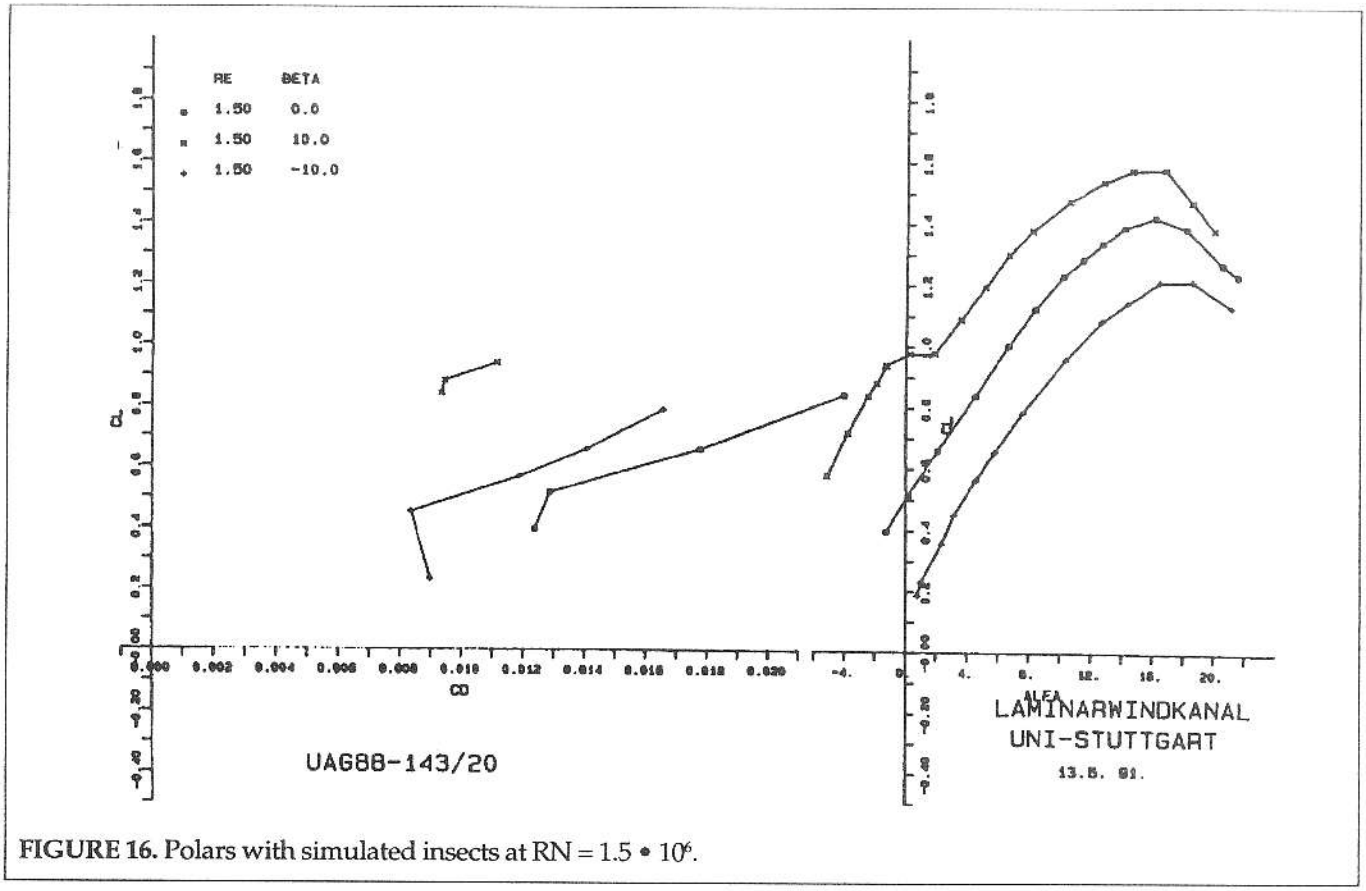

FIGURE 16. Polars with simulated insects at RN = 1.5 • 10^6.

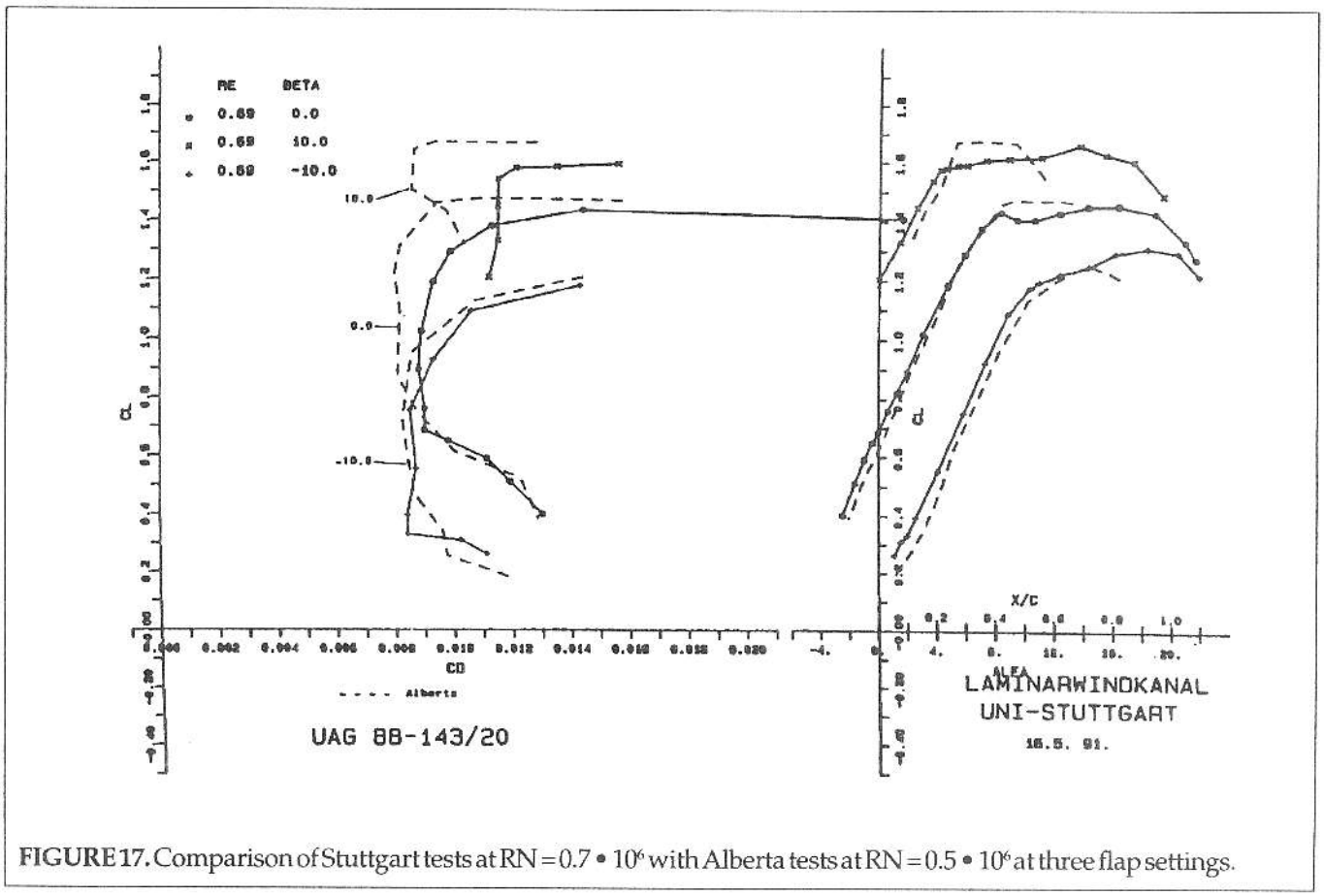

FIGURE 17. Comparison of Stuttgart tests at RN = 0.7 • 10^6 with Alberta tests at RN = 0.5 • 10^6 at three flap settings.

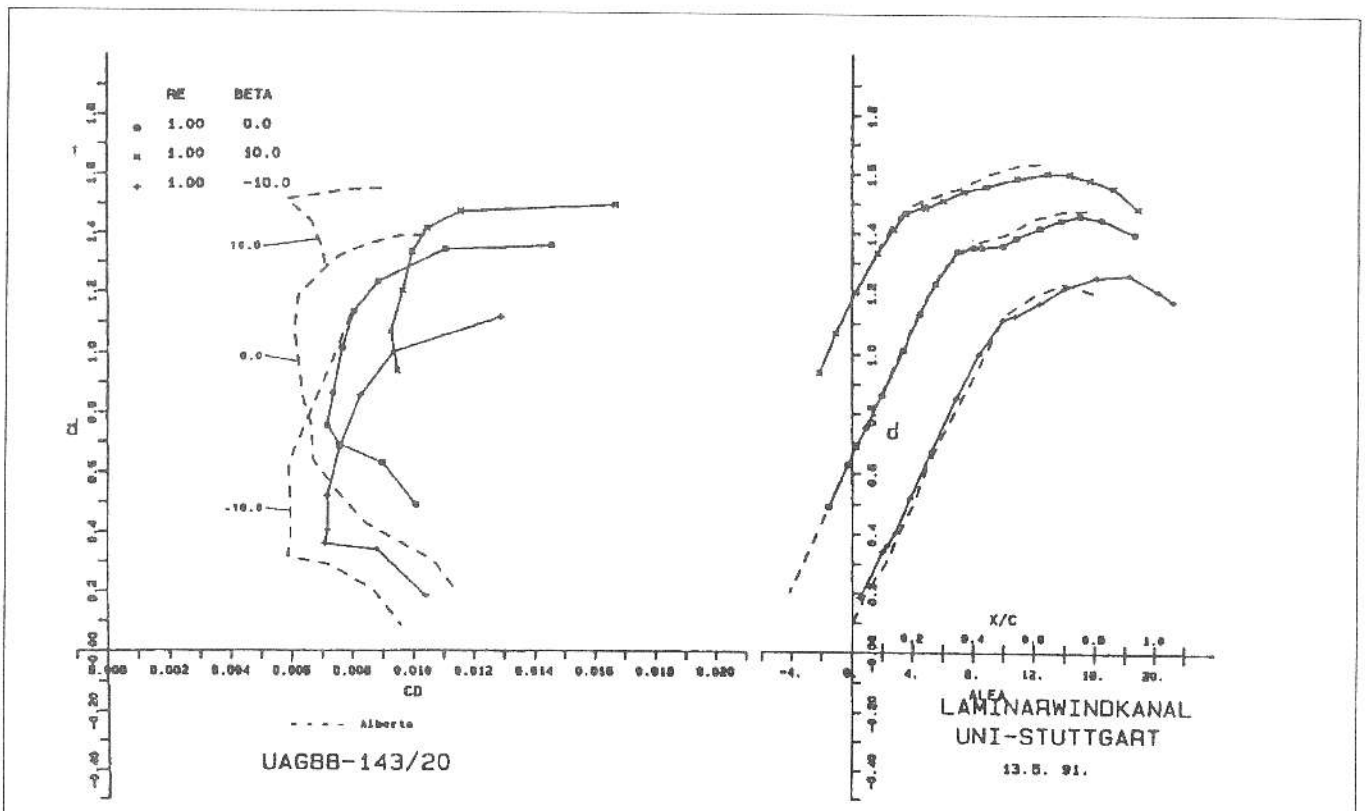

FIGURE 18. Comparison of Stuttgart tests with Alberta tests both at RN = 1.0 • 10^6 at three flap settings.

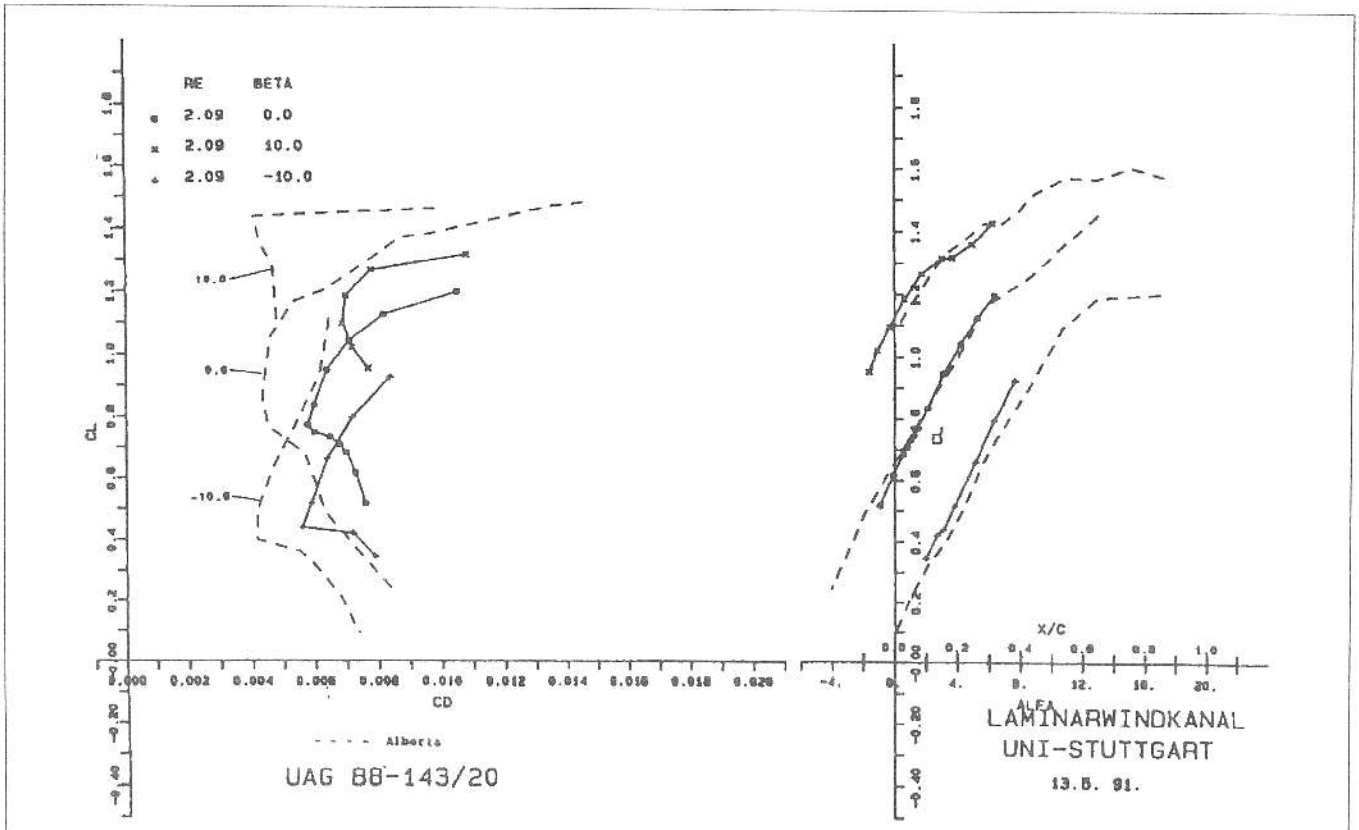

FIGURE 19. Comparison of Stuttgart tests with Alberta tests both at RN = 2.1 • 10^6 at three flap settings.

Figure 16 shows polars at RN = 1.5 • 10^6 for the model with the artificial insect pattern described above. The drag can only be measured in a small range of the lift with turbulent separation at higher lift. The lift curve slope is essentially smaller (refer to Figure13).

COMPARISON WITH ALBERTA MEASUREMENTS

The figures[2] were digitized to compare them with our tests. These coefficients are plotted together with the Stuttgart test results in Figures 17 to 19. Figure 17 shows the comparison of the Alberta tests at RN = 0.5 • 10^6 with the Stuttgart tests at RN = 0.7 • 10^6. There are drastic differences in the drag coefficients especially at zero, and positive flap deflections. This holds also for RN = 1.0 • 10^6 in Figure 18 and RN = 2.1 • 10^6 in Figure 19. There are only small differences in the C_L vs α polars but the maximum lift is somewhat higher in the Alberta tests.

The Alberta wind tunnel model has a span/chord ratio of 1.22, the ratio of the Stuttgart model is 1.46. Two-dimensional test conditions are ensured by suction through the tunnel walls in Alberta and by blowing along the walls in Stuttgart.

As demonstrated by flow visualization and marked in the figures large, laminar separation bubbles are present. These will be larger in the Stuttgart tests with a very low turbulence level. This is one cause for the higher drag coefficients.

Further reasons for the discrepancies are the different methods for evaluating the drag and lift coefficients. In Alberta the pressures are recorded one by one along the model surface or the wake. This is time consuming and in view of the very low free stream dynamic heads and, in the case of drag measurements, the large distance behind the trailing edge this will be worse. In the Stuttgart tests pressure distributions are integrated experimentally and are therefore immediately available without long delay.

Our experience during a long period of two-dimensional airfoil testing and the comparison with similar airfoil sections makes the Stuttgart results more reasonable. The comparison of results from the wind tunnel of the University of Delft with those of Stuttgart showed only small differences. As each wind tunnel will have its own peculiarities, only tests from the same tunnel should be taken as a scale.

When the UAG 88-143/20 airfoil is compared with the FX 67-K-150/17 airfoil data[7],as is done elsewhere[2], the Stuttgart test results of the UAG airfoil presented in this paper should be used.

SYMBOLS

c	airfoil chord
C_D	section profile-drag coefficient
C_L	section lift coefficient
C_M	section pitching-moment coefficient about quarter chord point
C_{MF}	flap pitching moment about its pivot point
RE,RN	Reynolds number based on free-stream conditions and airfoil chord
x	airfoil abscissa
y	airfoil ordinate
α	angle of attack relative to chord line,degrees
β	flap angle positive in downward direction

SYMBOLS USED IN ARTICLE

ACKNOWLEDGEMENTS

The authors are grateful to Dr.Mark Drela for the XFOIL design and analysis code.

REFERENCES

1. Dan M. Somers and Mark D. Maughmer: The SM701 Airfoil. Airfoils Incorporated,601 Cricklewood Drive, State College Pennsylvania 16803,December, 1990.
2. D. J. Marsden: Wind tunnel tests of an ultralight sailplane wing section. Presented at the XXI OSTIV Congress Wiener-Neustadt, Austria, (1989), *Technical Soaring*, Volume XIV, No. 1.
3. F. X. Wortmann u. D. Althaus: Der Laminarwindkanal des Instituts fur Aero- und Gasdynamik an der Technischen Hochschule Stuttgart ZfW 12 (1964), Heft 4.
4. D. Althaus: Drag measurement on airfoils. Paper presented at 17. OSTIV-Congress, Paderborn, 1981.
5. Mark Drela: XFOIL: An Analysis and Design System for Low Reynolds Number Airfoils. Preliminary Proceedings of the Conference on Low Reynolds Number Aerodynamics. Edited by Thomas J. Mueller, June, 1989, University of Notre Dame,Notre Dame, Indiana.
6. D. J. Marsden and R.W.Toogood: Wind tunnels tests of a slotted flapped wing section for variable geometry sailplanes. *Technical Soaring*, Volume XII, No.l.
7. D. Althaus u. F. X. Wortmann: Stuttgarter Profilkatalog I